Biologically Plausible Spiking Neural Networks for Perceptual Filling-In

Hadar Cohen-Duwek (hadar@nbel-lab.com)
Elishai Ezra Tsur (elishai@nbel-lab.com)

Neuro-Biomorphic Engineering Lab (NBEL), Department of Mathematics and Computer Science,
The Open University of Israel, Ra'anana, Israel

Abstract

Visual perception initiated with a low-level derivation of Spatio-temporal edges and advances to a higher-level perception of filled surfaces. According to the isomorphic theory, this perceptual filling-in is governed by an activation spread across the retinotopic map, driven from edges to interiors. Here we propose two biologically plausible spiking neural networks, which demonstrate perceptual filling-in by resolving the Poisson equation. Each network exhibits a distinct dynamic and architecture and could be realized and further integrated in the brain.

Keywords: cognitive architectures; computational perception; perception; vision; computational modeling; neural networks

Introduction

Visual perception initiates with low-level processing in the retina, from which it is propagated to the Lateral Geniculate Nucleus (LGN) and the primary visual cortex (V1). While in V1, visual data is transformed to represent Spatio-temporal edges (Marr, 1982), the perceived image has complete filled-in surfaces, suggesting that the brain reconstructs visual constructs from their edges (Von Der Heydt et al., 2009) (Figure 1).

Numerous visual phenomena shed light on the underlying neural mechanism of perceptual filling-in (Komatsu, 2006). Among them are the watercolor illusion (Pinna et al., 2001), the neon color spreading (Van Tuijl and Leeuwenberg, 1979), the Cornsweet illusion (Cornsweet, 1970), afterimage filling-in (Barkan and Spitzer, 2017; Van Lier et al., 2009) and the filling-in in the blind spot (Ramachandran, 1992). Extensive empirical research on these phenomena has led to two prominent theories governing perceptual filling-in (Komatsu, 2006): **(1) Symbolic or cognitive theory**, according to the contrast information at the surface edges is represented by low-level visual areas and the color and shape of the surface are described as metadata in higher areas; and **(2) Isomorphic theory**, according to perceptual filling-in, occurs as an activation pattern spreads across the retinotopic map of the visual cortex, from the surfaces' edges to interiors. This activation pattern propagates across a two-dimensional grid of neurons, representing a planar field of view.

The underlying mechanism of perceptual filling-in remains unclear, as there are experimental evidence supporting both hypotheses (Komatsu, 2006).

A recent computational model (Cohen-Duwek and Spitzer, 2018; Cohen Duwek and Spitzer, 2019) demonstrates many of the visual illusions, governed by perceptual filling-in, described above. The authors described a Poisson equation-based model, which can be used to reconstruct an image from its gradients. While the model describes a mathematical formulation for perceptual filling-in, it does not imply how and where it is realized with the visual system's neural activity.

In this work, we propose two neuronal implementations of the model proposed by Cohen-Duwek et al. (2018) using Spiking Neural Networks (SNN). These implementations support the isomorphic theory and demonstrate how biologically plausible neuronal models can lead to a perceived reconstruction of an image from its gradients. Particularly, we solve the Poisson equation by two distinct networks: (1) feedforward SNN in which a weight matrix was optimized to generate a solution (Figure 2, top); (2) Recurrent SNN, which follows evidence-based feedback connections, or horizontal connections (Gilbert and Wiesel, 1979; Hirsch and Gilbert, 1991) (Figure 2, bottom).

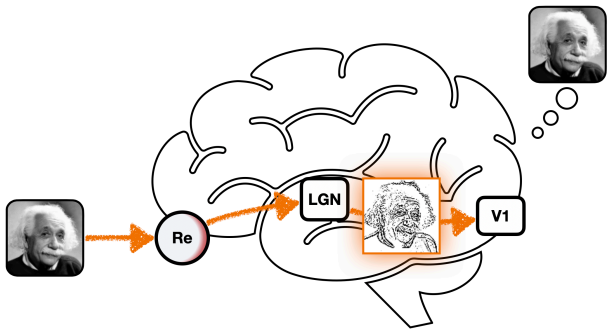

Figure 1: Illustration of perceptual filling-in. A perceived image is reconstructed from Spatio-temporal edges that emerged in V1 using surfaces' filling in. Image was modified form Miquel Perello Nieto; CC BY-SA 4.0.

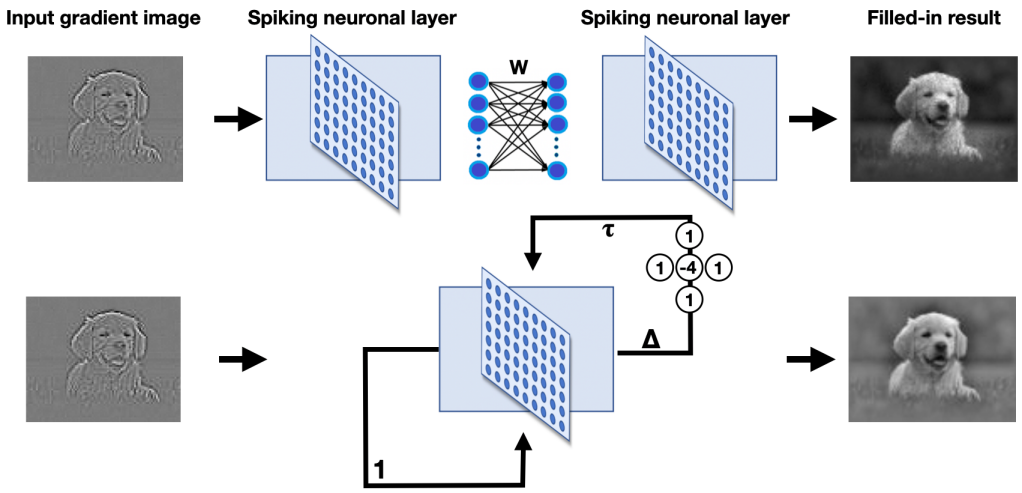

Figure 2: Two SNN architectures for perceptual filling-in. (top) Feedforward SNN. Dense connections of two spiking neuronal layers reconstruct an image from an input gradient image. (bottom) Recurrent SNN. Image is reconstructed iteratively over time through recurrent (horizontal) connections. Dog image by Hebrew Matio; CC BY-SA 4.0.

Methods

Filling-in model

The model proposed by (Cohen-Duwek and Spitzer, 2018, 2019) demonstrates a variety of filling-in illusions through the reconstruction of an image from its gradients by using the diffusion/heat equation:

$$\frac{\partial I_p}{\partial t} - \Delta I_p(x,y) = div(\nabla I_s), \quad (1)$$

where $\nabla = \left[\frac{\partial}{\partial x}, \frac{\partial}{\partial y}\right]$ is the gradient operator, $\Delta = \left[\frac{\partial^2}{\partial x^2} + \frac{\partial^2}{\partial y^2}\right]$ is the Laplacian operator, div is the divergence ($div\, \boldsymbol{F} = \frac{\partial F_x}{\partial x} + \frac{\partial F_y}{\partial y}$), I_p is the perceived image (i.e., the reconstructed image), and I_s is the input image (stimulus). With the diffusion model, the perceived image's surfaces are gradually filled in from edges to interiors.

In accordance with previous psychophysical reports, the perceived image is assumed to be reconstructed very fast (Barkan and Spitzer, 2017; Pinna, 2008; Van Lier et al., 2009) and was referred to as "immediate filling-in" (Von Der Heydt et al., 2009). Considering this fast dynamic, the dynamic phase of the diffusion equation $\frac{\partial I_p}{\partial t}$ can be ignored, reducing the diffusion equation to the steady-state Poisson equation:

$$\Delta I_p(x,y) = -div(\nabla I_s). \quad (2)$$

While the Poisson equation can be realized numerically by various techniques (Mikula, 2002; Simchony et al., 1990; Weickert, 1996), here, it is solved with SNNs.

Neural Engineering Framework

SNNs closely follow biological, computational principles. They were utilized to design a broad spectrum of neuromorphic (brain-inspired) frameworks ranging from robotic control (Zaidel et al., 2021) to visual processing (Tsur and Rivlin-Etzion, 2020). In this work, we utilized the Neural Engineering Framework (NEF) (Stewart and Eliasmith, 2014) for SNN design and optimization. NEF brings forth a theoretical framework for neuromorphic encoding of mathematical constructs with spiking neurons, allowing for the implementation of functional large-scale neural networks (Stewart and Eliasmith, 2014). It provides a computational framework with which information, given in terms of vectors and functions, can be transformed into a set of interconnected ensembles of spiking neurons. A version of NEF was compiled to work on both analog and digital neuromorphic hardware (Hazan and Ezra Tsur, 2021). In NEF, spikes train δ_i of neuron i in response to stimulus x is defined with:

$$\delta_i(x) = G_i\left[\alpha_i e_i + J_i^b\right], \quad (3)$$

where G_i is a spiking neuron model, α_i is a gain term, e_i is the neuron's preferred stimulus (encoding vector) and J_i^b is a fixed background current. An ensemble of neurons can encode a high-dimensional vector, which can be linearly decoded as $\hat{x}$ using:

$$\hat{x} = \sum_i^N a_i(x) d_i, \quad (4)$$

where N is the number of neurons, $a_i(x)$ is the postsynaptic low-pass filtered response of neuron i to stimulus x and d_i is a linear decoder that was optimized to reconstruct x using least squared optimization. As the number of neurons N

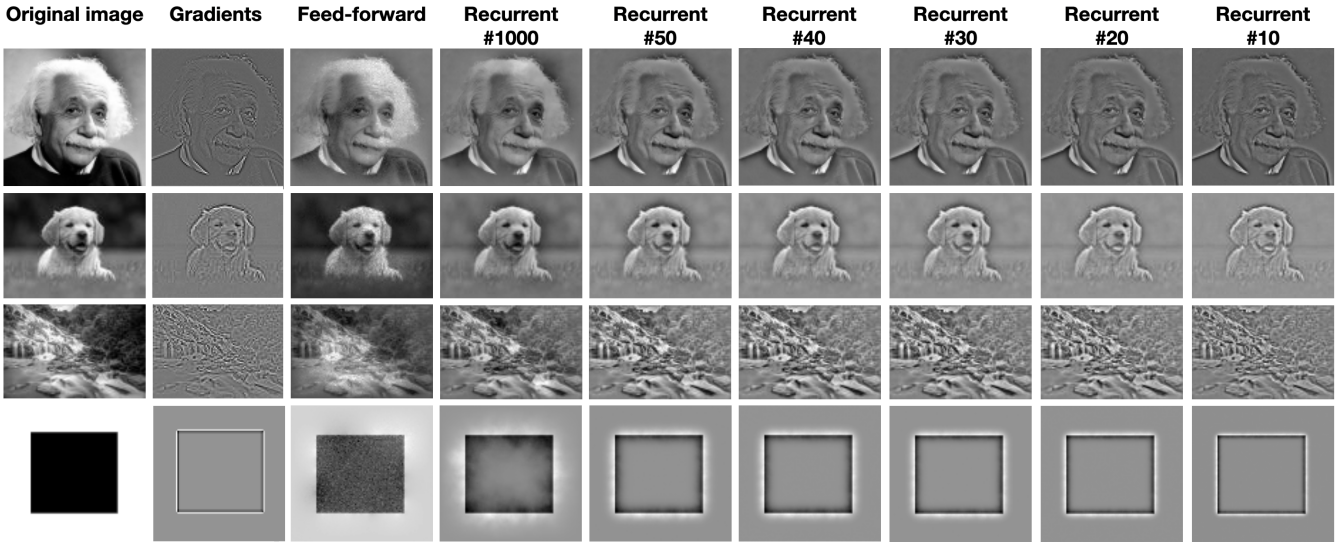

Figure 3: Simulation results. The original image and its Laplacian are at the 1st and 2nd columns, respectively. The results of the feedforward and recurrent (at iteration 1000) networks are at the 3rd and 4th columns, respectively. Recurrent methods at iteration 10-50 are at the 5th to 9th columns. Landscape image by BerryJ, Dog image by Hebrew Matio, Einstein photo by Miquel Perello Nieto, CC BY-SA 4.0.

increases, the mean squared error decreases as $1/N^2$. Neuron's postsynaptic response is defined using:

$$a_i(\mathbf{x}) = \sum_j h_i * \delta_i(t - t_j(\mathbf{x})), \tag{5}$$

where h_i is the synaptic response function (usually an exponential with a time constant τ determined by the neurotransmitter type at the synapse), "*" is the convolution operator, and $\delta_i(t - t_j(\mathbf{x}))$ is the spike train produced by neuron i in response to input $\mathbf{x}$, with spike times indexed by j.

Equations (3) and (4) describe how vectors are encoded and decoded using neural spiking activity in neuronal ensembles. Propagation of data from one ensemble to another is realized through weighted synaptic connections (Stewart and Eliasmith, 2014), formulated with a weighted matrix.

By integrating NEF's representation and transformation capabilities, we can realize intricate dynamic behavior by recurrently connecting neuronal ensembles. Particularly, NEF can be used to resolve a dynamic $dx/dt = f(x(t)) + u(t)$, where $u(t)$ is an input (the input can be from another neural population), by defining a recursive connection which resolves the transformation: $\tau \cdot f(x) + x$.

SNN architectures

Here, two NEF-based SNN architectures are proposed: 1) a feedforward SNN that solves the Poisson equation using a feedforward approach (Figure 2, top); and 2) a recurrent SNN that iteratively solves the Poisson equation using a recurrent approach (Figure 2, bottom).

Feedforward SNN

The feedforward SNN solves the Poisson equation by using matrix manipulations as follows. By using a finite difference numerical method (Volpert, 2014), the Poisson equation can be rewritten as a linear system:

$$A\vec{u} = \vec{b}, \tag{6}$$

where $\vec{u}_{mn\times 1}$ and $\vec{b}_{mn\times 1}$ are column vectors representing the pixels of the image $U_{m\times n}$ to be reconstructed and the edges (Laplacian) of the input stimulus, respectively (arranged in a natural ordering). $A_{mn\times mn}$ is the Laplace matrix defined with:

$$A_{mn\times mn} = \begin{bmatrix} D & -I & 0 & & 0 & 0 & 0 \\ -I & D & -I & \cdots & 0 & 0 & 0 \\ 0 & -I & D & & 0 & 0 & 0 \\ & \vdots & & \ddots & & \vdots & \\ 0 & 0 & 0 & & D & -I & 0 \\ 0 & 0 & 0 & \cdots & -I & D & -I \\ 0 & 0 & 0 & & 0 & -I & D \end{bmatrix}, \tag{7}$$

where $I_{n\times n}$ is the identity matrix and $D_{n\times n}$ is given by:

$$D_{n\times n} = \begin{bmatrix} 4 & -1 & 0 & & 0 & 0 & 0 \\ -1 & 4 & -1 & \cdots & 0 & 0 & 0 \\ 0 & -1 & 4 & & 0 & 0 & 0 \\ & \vdots & & \ddots & & \vdots & \\ 0 & 0 & 0 & & 4 & -1 & 0 \\ 0 & 0 & 0 & \cdots & -1 & 4 & -1 \\ 0 & 0 & 0 & & 0 & -1 & 4 \end{bmatrix}. \tag{8}$$

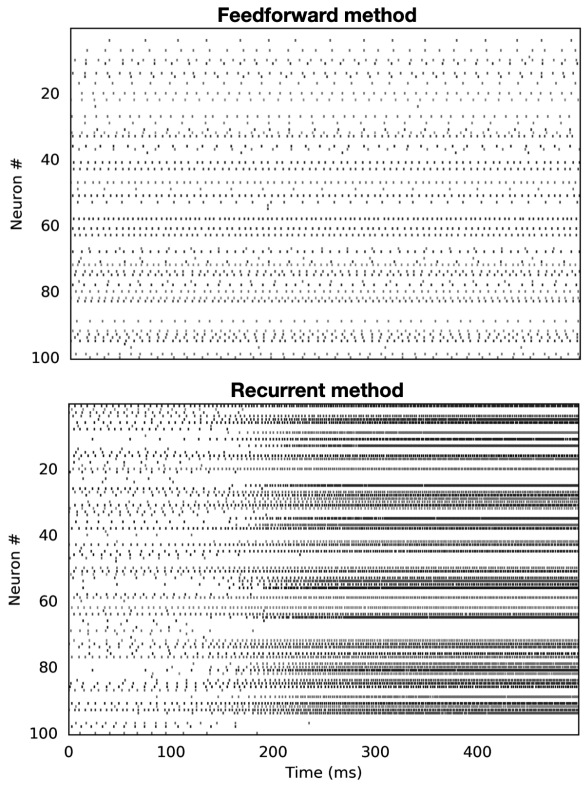

Figure 4: Raster plot for the black box image in the feedback (top) and the recurrent (bottom) methods. Spikes for the 100 neurons representing the central 5 pixels are shown (each pixel is represented by 20 neurons).

Note that A is composed of $m \times m$ blocks, each is a $n \times n$ matrix. D and I are $n \times n$ blocks. The size of A depends on the input dimensions. Here, we assume that the visual system is represented with a fixed $W_{mn \times mn}$, where $W = A^{-1}$, and the reconstructed image vector $\vec{u}$ can be calculated as follows:

$$\vec{u} = W\vec{b}. \tag{9}$$

This solution was implemented with a SNN by connecting two neuron ensemble layers with a weight matrix W (Figure 2, top). It should be noted that although A is a sparse matrix, W is not as sparse (A is not a block diagonal matrix, but rather a "tridiagonal with fringes" matrix) (Press et al., 1986). Accordingly, W represents an all-to-one connectivity scheme.

Recurrent SNN

The Recurrent SNN solves the Poisson equation iteratively by using the heat/diffusion equation dynamics. Rearranging the dynamic form of diffusion Eq. 1, as: $\frac{\partial I_p}{\partial t} = div(\nabla I_s) + \Delta I$, would allow us to define the feedback connection for the realization of the Poisson equation as:

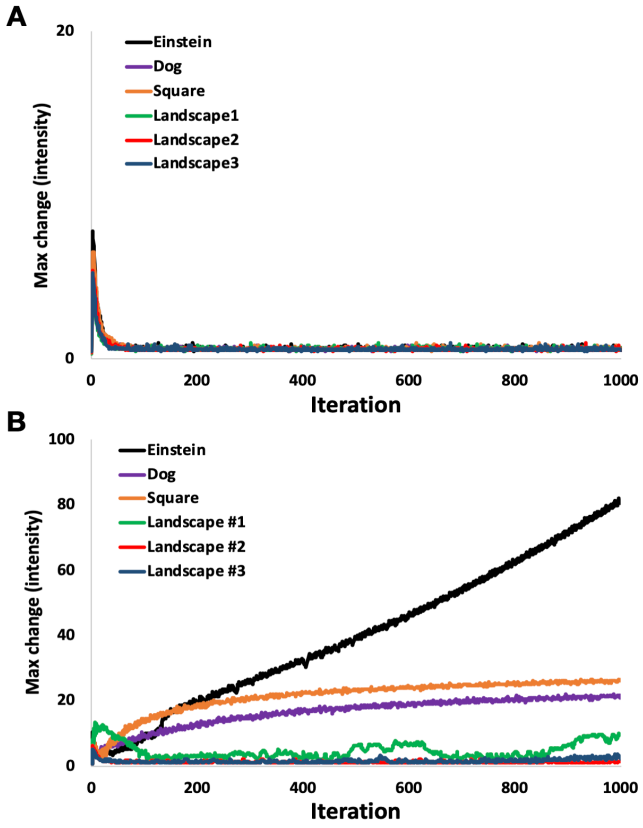

Figure 5: Convergence plot of the feedback method with 20 neurons per pixel (A) and with 10 neurons per pixel (B). x-axis represents the number of iterations and y-axis represents the maximum absolute difference between two sequential iterations. Only landscape 1 was shown in Figure 3.

$$feedback(I) = \tau \cdot (div(\nabla I_s) + \Delta I) + I, \tag{10}$$

which can be iteratively defined using:

$$I_k = \tau \cdot (div(\nabla I_s) + \Delta I_{k-1}) + I_{k-1}. \tag{11}$$

The recurrent method iteratively reconstructs the perceived image I_k for each time step k. This equation can be discretized using:

$$I_k = \tau \cdot \left(L(I_s) + L(I_{k-1})\right) + I_{k-1}, \tag{12}$$

where L is the discrete Laplace operator: $\begin{bmatrix} 0 & -1 & 0 \\ -1 & 4 & -1 \\ 0 & -1 & 0 \end{bmatrix}$.

A solution to Equation 12 for a perceived 2D $I(x,y)_k$ image, in which the value of a pixel in location (x,y) at time step k image is:

$$I(x,y)_k = \tau \cdot (div(\nabla I(x,y)_s) + I(x,y-1)_{k-1} + I(x,y+1)_{k-1} + I(x-1,y)_{k-1} + I(x+1,y)_{k-1} - 4 \cdot I(x,y)_{k-1}) + I(x,y)_{k-1}. \quad (13)$$

For each neuron, Equation 13 specifies four feedback connections to four neighboring neurons and one feedback connection to itself. In each time step k, neural activity is spread to the neuron's neighbors.

We implemented the recurrent Poisson solution using SNN with a single layer, where feedback connections were defined from the layer to itself. Therefore, this connectivity scheme can be referred to as horizontal connections (Gilbert and Wiesel, 1979; Hirsch and Gilbert, 1991) (Figure 2, bottom).

It should be noted that the recurrent method is not restricted to horizontal connections, as it can also be implemented with multiple neural layers. Thus, instead of horizontal connections, signals can be transmitted to a higher layer and then transferred back to the original layer with recurrent connections (top-down feedback loop).

Simulation and pre-processing

To evaluate our SNNs, we implemented them using the Nango neural compiler, with which high-level descriptions can be translated to low-level spiking neurons (Bekolay et al., 2014). The inputs to both simulations were the image Laplacian. The Laplace operator is commonly used as an approximation to the Difference of Gaussian (DOG) operator, representing the receptive fields of retinal ganglion cells (Marr, 1982). 10-20 spiking neurons encoded each pixel of the image's Laplacian with Spiking-Rectified-Linear activation function. Simulations were executed on an Azure virtual machine (6 cores, 56 GB RAM) and were accelerated by a GPU (Nvidia Tesla K80).

Results

We demonstrate both models' performance by comparing them with four different images (a photograph of Einstein, a dog, landscape, and black square). Figure 3 shows the original images, the image Laplacian (the divergence of the image gradients), and the resulted reconstruction (i.e., the perceived image) for both the feedforward and the recurrent methods shown.

Feedforward method

The results of the simulations are presented in Figure 3. The reconstructed images (the perceived images) are almost instantly reconstructed (or filled-in) from the image gradient (Laplacian). This filling-in process is rapid as the synaptic time constants determine its latency. The feedforward process's instantaneous nature is also demonstrated in Figure 4, top, where the neuronal activity is homogenous over time.

Recurrent method

In contrast to the feedforward method, the recurrent method requires numerous iterations to converged and reconstruct the image. Notably, convergence is also apparent in the neuronal activity, as shown in the raster plots presented in Figure 4 (bottom). The absolute maximal change across all pixels in the perceived image, over sequential iterations, is shown in Figure 5. Convergence is indicated when maximal change reduces to zero. To further realize the neuron number constraint, we monitored convergence, where the number of neurons representing a pixel reduced from 20 to 10 (Figure 5, A). It seems that with a small number of neurons, the solution diverges rather than converges, except the landscape image, which features long and continuous edges on many small surfaces (Figure 5, B).

Discussion

We introduced two biologically plausible computational methods in this work, which can serve as potential filling-in underlying neural mechanisms in the brain. Both methods were implemented using SNNs and were demonstrated with the reconstruction of an image from its Laplacian. Both methods are consistent with the isomorphic hypothesis since their resulted reconstruction was not directly stimulated by the input image.

Although both approaches solve the same equation, their neural mechanisms are distinctive. While the recurrent method iteratively solves the Poisson equation using a horizontal connectivity scheme (Figure 2, bottom), the feedforward method uses a weight matrix representing direct dense connectivity to do the same (Figure 2, top).

Several experimental findings support the spread of filling-in activities in V1 area. For example, Huang and Paradiso (2008), found that the response to a surface interior is delayed, relative to the response to the surface's edge, in a time constant proportional to the distance between a receptive field and the edge. Our recursive method is consistent with this result, as the surface's interior is filled in at a later iteration than the area near the edges (Figure 3). Thus, suggesting that the recursive method may emulate the filling-in process in V1.

As demonstrated by the black square example in Figure 3, filling-in is not complete for input images containing a large surface. This uncompleted filling-in phenomenon is consistent with experimental findings. For instance, Zweig et al., (2015), measured V1 responses to spatially uniform chromatic and achromatic squares using voltage-sensitive dye imaging in macaque monkeys. They found that V1 response to the center of the achromatic square increased with time, partially filling-in its center. Note that for small surfaces or input with multiple edges (such as a natural image with many small surfaces), the filling-in is completed, as no holes remain. It implies that natural images (with numerous edges) can be reconstructed at V1. This is also consistent with our findings, according to the filling-in of natural landscapes is less prone to neuronal resources. Both Zweig et al., (2015)

experimental findings and our model reveal an unfilled hole in the V1 area, suggesting that the recurrent model is insufficient to explain the neuronal representation of large uniform surfaces. Therefore, an additional mechanism might play a role in perceptual filling-in.

In contrast to the recurrent method, the feedforward is a non-iterative, direct method. Its filling-in performance is better than the recurrent method, as the hole in the center of the black square image example was filled. In terms of biological plausibility, the drawback of this technique is that it entails all-to-one connections (dense matrix). This implies that neurons at a higher layer are connected to almost every neuron at a lower layer. A dense connectivity scheme is inconsistent with the receptive field organization, often a characteristic of neuronal visual layers (Salin and Bullier, 1995). This biologically implausible architecture might be resolved by separating the visual field into distinct regions. Independent visual regions can be reconstructed (from their local gradients), and "stitched" together at a higher visual layer. Therefore, when searching for data to support a biologically plausible implementation of this method, we may wish to concentrate on higher visual areas. Indeed, experimental evidence for neural activity related to the filling-in process in the Cornsweet illusion, texture filling-in, and afterimage filling-in was found in V3 and V4 areas (De Weerd et al., 1995; Hong and Tong, 2017; Roe et al., 2005).

It is important to note that neither the recurrent nor feedforward mechanisms of perceptual filling-in can comprehensively explain the filling-in governed visual illusions. Filling-in illusions involve other neuronal processes, such as attention and lateral inhibition, beyond the current model's scope. The color dove, Cornsweet, and watercolor illusions, for example, involve the projection of contextual information by feedbacks (Devinck and Knoblauch, 2019). Therefore, feedback connections, which inhibit or induce neuronal activity in the V1 area, are required to predict these illusions. The mathematical model suggested by Cohen-Duwek et al. (2018, 2019) describes these illusions by using a weight function that reflects the neuronal processes by modifying the stimulus edges ahead of reconstruction. By utilizing SNNs, we may implement the neuronal lateral inhibition and feedback processes and compare the recurrent and feedforward approaches with experimental findings to better understand the underlying mechanism of perceptual filling-in.

Examining both approaches, the recurrent method represents a slow spread of neural filling-in activities in V1, whereas the feedforward method represents fast neural filling-in activities at higher visual areas. It might be possible that both approaches are present in the brain, where feedback represents slower computation of surfaces in lower visual areas, and the feedforward represents a faster reconstruction of surfaces in higher visual areas. The fast pathway might be involved in cognitive functions such as attention and learning. Notably, these cognitive functions are projected back via recurrent signals to modulate isomorphic processes in early visual areas (De Weerd, 2006; De Weerd et al., 2006; Herzog et al., 2016; Lin and He, 2012).

Acknowledgments

This work was supported by the Israel Innovation Authority (EzerTech) and the Open University of Israel research grant.

References

Barkan, Y., and Spitzer, H. (2017). *The Color Dove Illusion* (Vol. 1). Oxford University Press.

Bekolay, T., Bergstra, J., Hunsberger, E., DeWolf, T., Stewart, T. C., Rasmussen, D. and Eliasmith, C. (2014). Nengo: a Python tool for building large-scale functional brain models. Frontiers in neuroinformatics, 7, 48.

Cohen-Duwek, H., and Spitzer, H. (2018). A Model for a Filling-in Process Triggered by Edges Predicts "Conflicting" Afterimage Effects. *Frontiers in Neuroscience*, *12*, 559.

Cohen Duwek, H., and Spitzer, H. (2019). A compound computational model for Filling-in processes triggered by edges: watercolor illusions. *Frontiers in Neuroscience*, *13*, 225. h

Cornsweet, T. (1970). *Visual perception*. Academic Press.

De Weerd, P. (2006). Chapter 12 Perceptual filling-in: more than the eye can see. In *Progress in Brain Research* (Vol. 154, Issue SUPPL. A, pp. 227–245). Elsevier.

De Weerd, P., Gattass, R., Desimone, R., & Ungerleider, L. G. (1995). Responses of cells in monkey visual cortex during perceptual filling-in of an artificial scotoma. Nature, 377(6551), 731-734.

De Weerd, P., Smith, E., and Greenberg, P. (2006). Effects of selective attention on perceptual filling-in. *Journal of Cognitive Neuroscience*, *18*(3), 335–347.

Devinck, F., and Knoblauch, K. (2019). Central mechanisms of perceptual filling-in. In *Current Opinion in Behavioral Sciences* (Vol. 30, pp. 135–140). Elsevier Ltd.

Gilbert, C. D., and Wiesel, T. N. (1979). Morphology and intracortical projections of functionally characterised neurones in the cat visual cortex. *Nature*, *280*(5718), 120–125.

Hazan, A., & Ezra Tsur, E. (2021). Neuromorphic Analog Implementation of Neural Engineering Framework-Inspired Spiking Neuron for High-Dimensional Representation. Frontiers in Neuroscience, 15, 109.

Herzog, M. H., Thunell, E., and Ögmen, H. (2016). Putting low-level vision into global context: Why vision cannot be reduced to basic circuits. *Vision Research*, *126*, 9–18.

Hirsch, J. A., and Gilbert, C. D. (1991). Synaptic physiology of horizontal connections in the cat's visual cortex. *Journal of Neuroscience*, *11*(6), 1800–1809.

Hong, S. W., and Tong, F. (2017). Neural representation of form-contingent color filling-in in the early visual

cortex. *Journal of Vision*, *17*(13).

Huang, X., and Paradiso, M. A. (2008). V1 Response Timing and Surface Filling-In. *Journal of Neurophysiology*, *100*(1), 539–547.

Komatsu, H. (2006). The neural mechanisms of perceptual filling-in. In *Nature Reviews Neuroscience* (Vol. 7, Issue 3, pp. 220–231).

Lin, Z., and He, S. (2012). Emergent Filling In Induced by Motion Integration Reveals a High-Level Mechanism in Filling In. *Psychological Science*, *23*(12), 1534–1541.

Maass, W. (1997). Networks of spiking neurons: The third generation of neural network models. *Neural Networks*, *10*(9), 1659–1671.

Marr, D. (1982). *Vision: A computational investigation into the human representation and processing of visual information*. W. H. Freeman and Company.

Mikula, K. (2002). Image processing with partial differential equations. In *Modern Methods in Scientific Computing and Applications* (pp. 283–321). Springer Netherlands.

Pinna, B. (2008). Watercolor illusion. *Scholarpedia*, *3*(1), 5352.

Pinna, B., Brelstaff, G., and Spillmann, L. (2001). Surface color from boundaries: A new "watercolor" illusion. *Vision Research*, *41*(20), 2669–2676.

Press, W. H., Teukolsky, S. A., Vetterling, W. T., and Flannery, B. P. (1986). *Numerical Recipes: The Art of Scientific Computing*. Cambridge University Press.

Ramachandran, V. S. (1992). Blind spots. Scientific American, 266(5), 86-91.

Roe, A. W., Lu, H. D., and Hung, C. P. (2005). Cortical processing of a brightness illusion. *Proceedings of the National Academy of Sciences of the United States of America*, *102*(10), 3869–3874.

Salin, P. A., and Bullier, J. (1995). Corticocortical connections in the visual system: Structure and function. In *Physiological Reviews* (Vol. 75, Issue 1, pp. 107–154). American Physiological Society.

Simchony, T., Chellappa, R., and Shao, M. (1990). Direct Analytical Methods for Solving Poisson Equations in Computer Vision Problems. *IEEE Transactions on Pattern Analysis and Machine Intelligence*, *12*(5), 435–446.

Stewart, T. C., and Eliasmith, C. (2014). Large-scale synthesis of functional spiking neural circuits. In *Proceedings of the IEEE* (Vol. 102, Issue 5, pp. 881–898). Institute of Electrical and Electronics Engineers Inc.

Tsur, E. E., & Rivlin-Etzion, M. (2020). Neuromorphic implementation of motion detection using oscillation interference. Neurocomputing, 374, 54-63.

Van Lier, R., Vergeer, M., and Anstis, S. (2009). Filling-in afterimage colors between the lines. In *Current Biology* (Vol. 19, Issue 8).

Van Tuijl, H. F. J. M., and Leeuwenberg, E. L. J. (1979). Neon color spreading and structural information measures. *Perception & Psychophysics*, *25*(4), 269–284.

Volpert, V. (2014). *Elliptic Partial Differential Equations* (Vol. 104). Springer Basel.

Von Der Heydt, R., Friedman, H. S., and Zhou, H. (2009). Searching for the Neural Mechanism of Color Filling-In. In *Filling-In: From Perceptual Completion to Cortical Reorganization*. Oxford University Press.

Weickert, J. (1996). *Theoretical Foundations of Anisotropic Diffusion in Image Processing* (pp. 221–236).

Zaidel, Y., Shalumov, A., Volinski, A., Supic, L., & Tsur, E. E. (2021). Neuromorphic NEF-based inverse kinematics and PID control. Frontiers in Neurorobotics, 15.

Zweig, S., Zurawel, G., Shapley, R., and Slovin, H. (2015). *Representation of Color Surfaces in V1: Edge Enhancement and Unfilled Holes*.